Antibacterial filtration membrane based on PVDF-co-HFP nanofibers with incorporated medium-chain 1-monoacylglycerols

Journal:	*ACS Applied Materials & Interfaces*
Manuscript ID	am-2021-07257x.R2
Manuscript Type:	Article
Date Submitted by the Author:	n/a
Complete List of Authors:	Peer, Petra; Institute of Hydrodynamics Czech Academy of Sciences Janalikova, Magda; Tomas Bata University in Zlín Faculty of Technology, Department of Sedlarikova, Jana; Tomas Bata University in Zlin, Pleva, Pavel; Tomas Bata University in Zlin, Zelenkova, Jana; Institute of Hydrodynamics Czech Academy of Sciences, Filip, Petr; Institute of Hydrodynamics Czech Academy of Sciences, Opalkova-Siskova, Alena; Polymer Institute, Slovak Academy of Sciences; Institute of Materials and Machine Mechanics Slovak Academy of Sciences

Antibacterial filtration membrane based on PVDF-*co*-HFP nanofibers with incorporated medium-chain 1-monoacylglycerols

Petra Peer[a*], Magda Janalikova[b*], Jana Sedlarikova[c], Pavel Pleva[b], Petr Filip[a], Jana Zelenkova[a], Alena Opalkova Siskova[d,e]

[a]Institute of Hydrodynamics of the Czech Academy of Sciences, v. v. i., Pod Patankou 5, 166 12 Prague 6, Czech Republic

[b]Department of Environmental Protection Engineering, Faculty of Technology, Tomas Bata University in Zlin, Vavreckova 275, 760 01 Zlin, Czech Republic

[c]Department of Fat, Surfactant and Cosmetics Technology, Faculty of Technology, Tomas Bata University in Zlin, Vavreckova 275, 760 01 Zlin, Czech Republic.

[d]Polymer Institute, Slovak Academy of Sciences, Dubravska cesta 9, 845 41 Bratislava, Slovakia

[e]Institute of Materials and Machine Mechanics, Slovak Academy of Sciences, Dubravska cesta 9, 845 13 Bratislava, Slovakia

* Corresponding authors: peer@ih.cas.cz; mjanalikova@utb.cz

Abstract:

The efficiency of filtration membranes is substantially lowered by bacterial attachments and potential fouling processes, these reduce their durability and lifecycle. The antibacterial and antifouling properties exhibited by used materials play a substantial role in their application. We tested a material based on electrospun copolymer poly(vinylidene fluoride)-*co*-hexafluoropropylene (PDVF-*co*-HFP) where incorporated was an agent with a small amount of ester of glycerol consecutively with caprylic, capric, and lauric acids. Each of these three materials differing in used esters (1-monoacylglycerol, 1-MAG) was prepared in three weighted concentrations of 1-MAG (1, 2, and 3 wt%). The presence of 1-MAG with an amphiphilic structure resulted in the prepared materials´ hydrophilic character that contributed to filtration performance. The tested materials (membranes) were characterized with rheological, optical (SEM), FTIR, XRD, and other methods to evaluate antibacterial and antifouling activities. The pure water flux was six times higher than that of the neat PVDF-*co*-HFP membrane when the 1-MAG addition attained only 1 wt%. It was experimentally shown that the PVDF-*co*-HFP/1-MAG membrane with high wettability improved antibacterial activity and antifouling ability. This membrane is highly promising for water treatment due to the safety of antibacterial 1-MAG additives.

KEYWORDS: nanofibrous membranes, monoacylglycerols, poly(vinylidene fluoride)-*co*-hexafluoropropylene, antibacterial activity, antifouling activity, wettability, filtration.

1. Introduction

Microbial contaminations represent a serious problem for the practical application of packaging, biomedical devices, textile, and cosmetic products. In membrane technology, biofouling characterized as a nonspecific surface attachment of different kinds of microorganisms, can reflect in the reduced durability of membranes and the deterioration of their efficiency.

In the recent period this branch has been very strongly and positively influenced by the massive application of electrospun materials. Classical filtration membranes made of traditional polymer- and ceramic-based materials have been gradually replaced by the new porous electrospun materials characterized by an extremely high surface-to-volume ratio and relatively cheap production costs. Among them, fluoropolymers such as poly(vinylidene fluoride) (PVDF) represent a promising material.[1,2] PVDF exhibits high mechanical strength, increased chemical resistance, excellent thermal stability, and high hydrophobicity. If hexafluoropropylene (HFP) groups are incorporated into PVDF, then the resulting copolymer PVDF-*co*-HFP exhibits even better mechanical strength, lower crystallinity, higher solubility, greater free volume, and higher hydrophobicity. All these properties predetermine PVDF-*co*-HFP as a very promising material in membrane production.[3-5]

However, in spite of these favorable properties, problems such as fouling, pore wetting, and microbial accumulation persist. Higher hydrophobicity represents an unwanted phenomenon in some applications because materials cause fluids to accumulate, which leads to very moderate or no wound healing.[6] The classic approach to overcome the problems of electrospun PVDF-*co*-HFP membranes mentioned above is to apply metal nanoparticles such as Ag[7], ZnO[8,9], TiO_2[10], CuO[11]. The presence itself of metal nanopowders is not as decisive as their morphology within the copolymer nanofibers. There are three possibilities of how to incorporate nanopowders into (onto) the fibers[12]: (i) they are mixed with the copolymer prior to the electrospinning process and then distributed across the whole volume; (ii) the resulting nanofibrous filters are produced by copolymer electrospinning in combination with nanopowder electrospraying; (iii) nanopowder rich surface is obtained by coaxial electrospinning. For the case of ZnO, it was shown[8,9] that the processing "on" (decoration of fibers with ZnO) provides better antibacterial results than the processing "in". Modification of membranes incorporating various organic or inorganic materials have been used to improve different properties, such as antibacterial and anti-fouling effects[13-15], hydrophilicity increase, improvements of the water flux, the rejection capacity of compounds and structural membrane parameters.[16]

On the other hand, it is well known that the toxicity of nanoparticles is more significant than the toxicity of larger particles of the same materials, even for materials with relatively low toxicity.[17] This fact is also a driver seeking alternative possibilities for replacing the usage of nanopowders. Owing to the excellent mutual compatibility of mixed multi-arm amphiphilic fluxible poly(*p*-phenylene terephthalamide) (f-PPTA) with pure PVDF, the electrospun membrane did not suffer from washing away as in the case of hydrophilic polymers or inorganic nanoparticle aggregation.[18] The exhibited antifouling and antibacterial activities were very promising.

The efficiency of fatty acids and derivatives as antimicrobial agents has been proven for a long-term period.[19,20] Generally, they exhibit both bacteriostatic (growth-inhibiting) and bactericidal (killing) effects. Contrasting to synthetic materials, they are amply present in nature. The present authors studied[21] the antibacterial efficiency of membranes electrospun from poly(vinyl butyral) (PVB) to which low concentrations of selected 1-monoacylglycerols (1-MAG) were added. The results justified a choice of 1-MAG as a suitable material in combination with PVB. The antimicrobial properties of 1-MAGs depend on the given molecular structure, i.e. the type and the length of a fatty acid carbon chain. They interfere with bacterial cell membranes and might cause cell lysis or a range of indirect effects inhibiting cell metabolism.[20]

Based on this result, the aim of this study is to analyze antibacterial and antifouling efficiency of the membranes electrospun from copolymer PVDF-*co*-HFP with the addition of three different 1-monoacylglycerols destabilizing bacterial cell membranes, specifically monocaprylin (1-MAG C8:0), monocaprin (1-MAG C10:0), and monolaurin (1-MAG C12:0). All three PVDF-*co*-HFP/1-MAG membranes were systematically characterized, and the activity of concentration of various 1-MAG types on the antibacterial (*S. aureus* and *E. coli*) and antifouling properties is described.

To this aim, several experimental techniques were consecutively used: characterization of polymer solutions, such as rheometric measurements, surface tension, viscosity and conductivity, as they strongly influence morphology of the produced membranes. Surface properties were analyzed as they affect the susceptibility to fouling mechanisms and thus, the filtration performance. Structural and morphological properties were evaluated to verify the potential interactions between polymer and active monoacylglycerols.

It will be shown that even a negligibly small amount of 1-MAG (1 wt%) facilitates the process of copolymer electrospinning and also participates in improving surface quality of electrospun membranes. In contrast to the neat copolymer PVDF-*co*-HFP, the adding of 1-MAG projects much higher antifouling and antibacterial efficiency of electrospun membranes.

2. Materials and Methods

2.1. Materials, chemicals, and microorganisms

PVDF-*co*-HFP Kynarflex® (copolymer poly(vinylidene fluoride)-*co*-hexafluoropropylene) was purchased from Arkema (Colombes, France) and dissolved in N,N´- dimethylformamide (DMF) (p.a.) from P-LAB (Prague, Czech Republic). The caprylic, capric, and lauric acid, glycidol, and chromium acetate hydroxide were supplied by Sigma-Aldrich (St. Louis, MO, USA). All the chemicals were utilized as received without further purification. Both of the bacterial strains - Gram-positive cocci of *Staphylococcus aureus* ATCC 25923 and Gram-negative rods of *Escherichia coli* ATCC 25922 - were obtained from the Czech Collection of Microorganisms (CCM, Brno, Czech Republic).

2.2. Preparation of the 1-MAG variants

Three saturated medium-chain fatty acids were applied in the preparation of antibacterial agents: caprylic acid $CH_3(CH_2)_6COOH$ (C8:0), capric acid $CH_3(CH_2)_8COOH$ (C10:0), and lauric acid $CH_3(CH_2)_{10}COOH$ (C12:0). The letter *x* in Cx:y denotes the amount of carbon atoms in the corresponding fatty acid, while *y* indicates a number of double bonds (0 in the case of saturation). The esters tested for destabilization of the bacterial cells of the membranes comprised monocaprylin (1-MAG C8:0), monocaprin (1-MAG C10:0), and monolaurin (1-MAG C12:0). The authors prepared 1-monoacylglycerols of the acids[22] by directly adding the given fatty acid into glycidol via the epoxide ring opening, this occurring in a double wall reactor at 90°C. The product was then recrystallized from ethanol at 99% purity. The structure of the 1-MAG utilized is shown in Fig. 1.

Note: For the sake of brevity and simplicity, 1-MAG Cx:y is hereinafter referred to as MAG x.

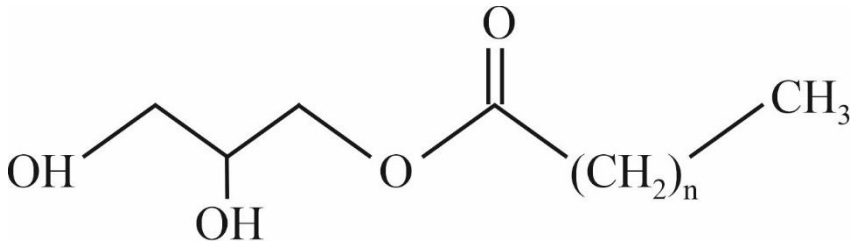

Figure 1. Chemical structure of the MAG variants: monocaprylin (MAG 8, n=6), monocaprin (MAG 10, n=8), and monolaurin (MAG 12, n=10).

2.3. Preparation of the nanofibrous membranes

The nanofibrous membranes were fabricated by electrospinning. Initially, PVDF-*co*-HFP was dissolved in DMF at a concentration of 23 wt% with the differing amounts of MAG (1, 2, and 3 wt%). A magnetic stirrer (Heidolph, Schwabach, Germany; set to 250 rpm at 25°C) was applied to homogenize the solutions over 24 hours. The subsequent nanofibrous webs were spun on a needle-less device consisting of a high voltage power supply (Spellman SL70PN150, Hauppauge, NY, USA), a carbon steel stick (10 mm in diameter) with a hemispherical hollow at the top, and a motionless, grounded, flat, metal collector. The operating parameters for electrospinning were as follows: the voltage was set to 18 kV, the tip-to-collector distance equaled 15 cm, and humidity and temperature were maintained at 35±1 % and 25±1 °C, respectively. Approximately 0.8 mL of polymeric solution was used in total for preparing the given membranes, and the entire electrospinning process did not exceed 16 minutes for each sample.

2.4. Characterization of the polymer solutions

Rheological measurements were carried out using a Physica MCR 501 rotational rheometer (Anton Paar, Graz, Austria), equipped with concentric cylinders (inner/outer diameters - 26.6/28.9 mm) at the constant temperature of 25°C. The conductivity of the PVDF-*co*-

HFP/MAG solutions was discerned on a Conductivity Meter Lab 960 unit (SCHOTT Instruments, Mainz, Germany) at 24°C. Surface tension was determined via the Wilhelmy plate method (10 × 19.9 × 0.2 mm) on a Krüss K 100 force tensiometer (Krüss GmbH, Hamburg, Germany) at 25°C.

2.5. Characterization of the nanofibrous membranes

The surface morphology of the nanofibers was investigated on a scanning electron microscope VEGA 3 (SEM, Tescan, Brno, Czech Republic) at a voltage of 10 kV and working distance of 7.5 mm. Prior to SEM observations, the samples were sputtered with a layer of gold (on a Quorum Q150R sputter device, Quorum Technologies Ltd, UK). The arithmetic means for fiber diameter were determined in Adobe Creative Suite software (CS5, Adobe Systems Inc., San Jose, CA, USA). To this aim, 300 individual fibers from 3 different SEM images were analyzed. Pore size distribution was ascertained concurrently, and calculation of mean pore size was based on more than 30 values.

The wettability of the nanofibrous membranes was gauged by determining contact angles, in accordance with the static sessile drop technique, on a Surface Energy Evaluation System by Advex Instruments (Brno, Czech Republic) at room temperature. A water droplet was placed on the fibrous surface by a syringe, and the water contact angle (WCA) was measured 3 seconds after its placement. Mean values were calculated from five independent measurements with demineralized water as the reference liquid; the volume of each deposited droplet equaled 3 μL.

The chemical composition of the nanofibrous membranes was characterized by Fourier transform infrared spectroscopy (FTIR) on a Nicolet 6700 spectrometer (ThermoFisher Scientific, Waltham, MA, USA) set to ATR mode, the range of 4000 to 400 cm^{-1}, and resolution of 2 cm^{-1}. The amount of β and γ phases was calculated according to Equation 1:

$$P\ (\beta + \gamma) = 100 \times \frac{A_{\beta,\gamma}}{1{,}26A_{\alpha} + A_{\beta,\gamma}}, \quad (1)$$

where A_{α} and $A_{\beta,\gamma}$ represent values for absorbance at 763 cm^{-1} and 840 cm^{-1}, respectively. The exclusive β phase peak at 1275 cm^{-1} and γ phase peak at 1234 cm^{-1} were applied to determine the content of the phases separately.[23]

X-ray diffraction analysis of the electrospun PVDF-*co*-HFP and PVDF-*co*-HFP/MAG 12 (2 wt%) samples was performed on a D8 DISCOVER diffractometer (Bruker, Karlsruhe, Germany). The device was equipped with an X-ray tube and rotating Cu anode operating at 12 kW. Parallel beam geometry with a parabolic Goebel mirror in the primary beam was employed for all measurements. Recordings were taken of X-ray diffraction patterns in the setting for grazing incidence and at the angle of incidence of $\alpha = 4°$.

2.6. Filtration test

Filtration experiments were conducted on PVDF-*co*-HFP/MAG samples that had been electrospun (the thickness of the layer equaling 30 ± 3 μm) onto a viscose non-woven textile (at the thickness of 250 ± 12 μm), the latter serving as a substrate to obtain a structure with good mechanical properties. The permeation fluxes of the membranes were determined on a dead-end filtration system (Model GV 025/2, Whatman, Maidstone, UK) under the transmembrane pressure of 4 bar. Deionized water was utilized in the tests. The permeation flux F [L m^{-2} h^{-1}] was calculated as follows:

$$F = \frac{V}{At} \ , \qquad (2)$$

where V is permeation volume (100, 500, 1000 mL) over the interval t [h], and A is the effective area of the filter membrane [m^2].

2.7. Antibacterial activity

Antibacterial activity was observed by three different methods – a) disk diffusion method, b) shake flask procedure, and c) the contact method.

a) As the first step, the antibacterial activity of the MAG variants was tested by standard agar disk diffusion technique.[24] Sterile disks (diameter 9 mm, Whatman, Maidstone, UK) were impregnated with the solution of the active 20 μL substance (the concentration corresponding to 5 wt% in ethanol), which were then placed on Mueller Hinton agar plates (Himedia Laboratories Pvt. Ltd., Mumbai, India) inoculated with 1 mL of 0.5 McF turbid bacterial suspension (*Staphylococcus aureus*, *Escherichia coli*) in sterile saline solution. The plates were incubated at 36±1°C for 24±1 h. The inhibition zones and bacterial growth under the samples were valuated. The same procedure was applied for circular samples (9 mm in diameter) of the neat PVDF-*co*-HFP and the PVDF-*co*-HFP copolymer which had been supplemented with MAG nanofibrous membranes prior to placement on agar plates. All experiments were repeated in triplicate.

Agar diffusion tests were also carried out with the PVDF-*co*-HFP and PVDF-*co*-HFP/MAG membranes on non-woven textile subsequent to the filtration experiment (2.6). Disk-shaped samples (25 mm in diameter) were placed on the agar inoculated with the aforementioned bacterial suspension (*Staphylococcus aureus, Escherichia coli*).

b) A modified[25] version of the standard flask shaking method was applied as a parallel procedure for evaluating antibacterial activity. Samples of the PVDF-*co*-HFP or PVDF-*co*-HFP/MAG nanofibers on aluminum foil (disks of diameter 25 mm) were added into 100 mL flasks (Duran, DWK, Mainz, Germany) containing 25 mL of sterile saline solution and bacteria (*S. aureus, E. coli*) at the concentration of 5x10^5 – 1x10^6 CFU.mL^{-1}. The mixtures were shaken at 100 rpm on a shaking incubator at 36±1°C. Viable counts of bacteria present in the solution were determined at the required contact intervals (60, 120, 300, and 1440 min.) by the spiral plate method (Eddy JetIUL, Barcelona, Spain); the experiment was performed in triplicate. Equation 3 was applied to calculate the rate of reduction in percent (% R):

$$\% R = 100 \times \frac{B - C}{B} \quad , \tag{3}$$

where B is the number of bacteria initially present in the bacterial solution before adding the nanofibers (control), and C is the number of bacteria present in the solution after the desired contact time (sample).

c) The contact technique was carried out according to ISO 22196: 2011[26] against *S. aureus* and *E. coli*. The specimens were sterilized first under UV light for 60 minutes, then 400 µL of the bacterial suspension (ranging in concentration between $2.5x10^5$ and $1x10^6$ cells.mL^{-1}) were loaded onto each nanofibrous sample (50 x 50 mm in size), which was subsequently covered with a square-shaped piece of polyethylene film (40 × 40 mm). After the contact interval of 24±1 h at 35±1°C and minimum relative humidity of 90%, the samples were rinsed with 10 mL of soybean casein digest broth with lecithin polyoxyethylene sorbitan monooleate (SCDLP broth). Bacterial counts (CFU.mL^{-1}) were conducted, and values for reduction in the number of living and viable cells of the tested bacteria (R) were calculated by Equation 4 below[26]:

$$R = (U_t - U_0) - (A_t - U_0) \quad , \tag{4}$$

where U_t is the mean of the common logarithm of the viable bacteria count in cells.cm^{-2} recovered from the neat PVDF-*co*-HFP control samples after 24±1 h; U_0 is the mean of the common logarithm of the viable bacteria count in cells.cm^{-2} recovered from the PVDF-*co*-HFP/MAG control samples immediately after inoculation; A_t is the mean of the common logarithm of the viable bacteria count in cells.cm^{-2} recovered from the PVDF-*co*-HFP/MAG 12 test samples after 24±1 h.

2.8. Antifouling activity

The antifouling activity of the membranes was determined by a modified bacterial adhesion test[11,27] as follows: 100mL glass bottles were used (Duran, DWK, Germany) containing 25 mL of sterile saline solution, bacteria (*S. aureus* or *E. coli*) at the final concentration of ~$5x10^5$ CFU.mL^{-1}, and the sample (PVDF-*co*-HFP or PVDF-*co*-HFP/2 wt% MAG 12 nanofibrous membranes; aluminum foil constituted the control) as a circular disk (diameter 25 mm). All the flasks were incubated at 36±1°C for 72±1 h. The membranes were then taken out of the solution, washed, immersed into sterile saline solution in conical tubes, and underwent vigorous vortexing for 20 minutes to dislodge bacteria from the nanofiber surfaces into the solution. Counts of viable sessile cells were determined by the spiral plate method described earlier and expressed as Log CFU.mL^{-1}. Consequently, ratios for bacteria killing (logarithmic reductions) were calculated by comparing and subtracting the bacterial counts for PVDF-*co*-HFP and PVDF-*co*-HFP/MAG from the pure aluminum foil as the control. Three measurements were used to determine the average.

2.9. Biofilm formation test – SEM and fluorescence microscopy

The capacity for bacterial attachment and biofilm formation on the surface of the PVDF-*co*-HFP and PVDF-*co*-HFP/MAG nanofibrous membranes were studied by two microscopy techniques. Circular samples (9 mm disks) cultured in BHI broth (Himedia Laboratories Pvt. Ltd., Mumbai, India) were supplemented with 5% v/v sucrose (Merck, Darmstadt, Germany) and *S. aureus* or *E. coli.* Cultivation at 37°C lasted for 72 h, after which the samples were made ready for the microscopy analyses.

a) Following cultivation, the samples were washed with sterile saline solution and put on a slide, where they were dyed with fluorescence dye (SYTO®9 and propidium iodide) for 10 s and covered with a square coverslip. Fluorescence microscopy was performed on an Olympus BX53 fluorescence microscope (Olympus, Tokyo, Japan), equipped with a DP73 Microscope Digital Camera (Olympus, Tokyo, Japan) and running cellSens Standard 1.18 software (Olympus, Tokyo, Japan). Analysis was carried out in a minimum of 20 positions in triplicate. The LIVE/DEAD™ BacLight™ Bacterial Viability Kit (Thermo Fischer, USA) was employed with slight modification following the protocol.[28] The SYTO®9 dye highlights all bacteria, while the propidium iodide only colors the DNA of dead cells; the excitation and emission maxima for the dyes are ca 480/500 nm for the SYTO®9 stain and 490/635 nm for the other. Thus, bacteria with intact cell membranes are picked out in fluorescent green, whereas bacteria with damaged membranes (dead) are stained fluorescent red.

b) The sample disks were washed after cultivation with sterile saline solution and left to dry at 40°C. SEM microscopy was then performed as described earlier (Subsection 2.5.).

2.10. Statistical analysis

Data were expressed as mean ± standard deviation (SD). Statistical analysis was conducted by the one-way ANOVA (ANalysis Of VAriance test) test commonly used to compare three or more groups of data by Statistica software (version 10, StatSoft, Inc., Tulsa, OK, USA) at the significance level of $p < 0.05$. Various letters mean that there are statistically significant differences between the compared data.

3. Results

3.1. Characterization of the polymer solutions

PVDF-*co*-HFP is a commercial semi-crystalline polymer commonly used to fabricate nanofibers that possesses excellent properties, such as high strength and superior resistance to a broad spectrum of chemicals.[29] Various solvents can be applied in PVDF-*co*-HFP electrospinning, such as acetone, DMF, tetrahydrofuran, and a mixture of these solvents.[8,30,31] Pure DMF was found in the present study to be suitable for electrospinning PVDF-*co*-HFP. Based on findings of previous work by the authors[31], a fixed concentration of PVDF-*co*-HFP

in DMF (23 wt%) was chosen to fabricate the circular, beadless nanofibrous membranes described herein.

Systematic investigation took place of the effect exerted by MAG concentration on the parameters of the solution, e.g. conductivity, surface tension, and viscosity, aspects which significantly alter the morphology[32] of the electrospun nanofibers. It is known that the surface tensions of the solution have to be overcome during the initial phase of the electrospinning process. Numerous attempts have been made to decrease the surface tension and obtain a fibrous structure with a lower level of defects.[33] Table 1 summarizes the findings on surface tension and conductivity for all the prepared solutions. The values for the surface tensions of the various PVDF-*co*-HFP solutions were relatively low, ranging from 36 to 38 mN/m. The primary factor in this pertains to the character of the solvent, DMF in this case, which attains relatively low surface tension (about 35 mN/m).[34] No significant change was initiated by increasing the concentrations of the MAG variants, in agreement with a published study[23] which investigated 20 wt% PVDF in dimethylsulfoxide/acetone solvents (36.6 mN/m) enriched with hexadecyltrimethyl ammonium bromide (35.5 mN/m). Regarding the conductivity of the solutions, the values between the types of MAG differed, albeit only by a little. The cause was the non-ionic nature of the applied MAG variants. A diverse trend was observed in another study[35], where poly(vinyl alcohol) based nanofibers were enriched with cationic benzyl triethylammonium chloride. Therein, a significant increase in conductivity brought about a collision of fibers followed by the formation of aggregates.

Table 1. Dependence of surface tension and electrical conductivity on MAG concentration in the PVDF-*co*-HFP solutions.

c [wt%]	Surface tension [mN/m]			Conductivity [μS/cm]		
	MAG 8	MAG 10	MAG 12	MAG 8	MAG 10	MAG 12
0	37.77±0.75^{a}			7.40±0.01^{a}		
1	37.33±0.15^{a}	37.57±0.38^{a}	37.60±0.30^{a}	6.68±0.08^{b}	8.34±0.05^{b}	7.28±0.08^{b}
2	37.17±0.25^{a}	37.63±0.25^{a}	37.73±0.21^{a}	6.56±0.05^{c}	8.12±0.08^{c}	7.12±0.08^{c}
3	36.20±0.36^{b}	37.27±0.25^{a}	36.87±0.21^{b}	6.26±0.05^{d}	8.46±0.05^{d}	6.92±0.04^{d}

The lower-case letters in the columns denote significant differences ($p<0.05$).

The apparent viscosity of the polymer solutions is affected by the molecular weight and concentration of the polymer, the nature of the solvent, and the additives employed.[36] As shown in Figure 2, shear viscosity exhibits a trend of a very moderate decrease in parallel with a rise in MAG concentration. This behavior was predictable due to non-cooperative binding between the PVDF-*co*-HFP chain and MAG.[37] As viscosity diminishes through the

presence of the surfactant, the nanofibers provide more even morphology of fibers.[38] As a consequence of the non-ionic character of the surfactant, no significant variation in the trend for viscosity was expected.[38] Measurements for viscosity were carried out in triplicate, and negligible deviation was observed - as expected for this type of rheometric measurement.

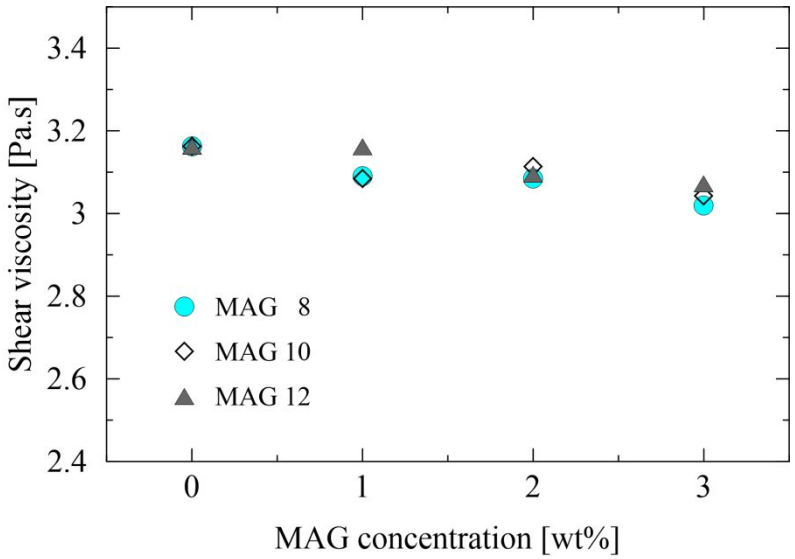

Figure 2. Shear viscosity of the neat PVDF-*co*-HFP and PVDF-*co*-HFP/MAG solutions.

3.2. Characterization of the nanofibrous membranes

Fiber diameter and pore size are important parameters that affect the functional properties of a filtration membrane, which is why SEM analysis was employed to discern the effects of concentration and the MAG variants on the morphology of the fibers. The PVDF-*co*-HFP solutions with various concentrations of MAG were electrospun to obtain the composite nanofibrous membranes. The circular cross-sections in Figure 3a detail the beadless morphology of the neat PVDF-*co*-HFP nanofibers. Adding MAG to the neat copolymer contributed in two ways: firstly, the electrospun beadless nanofibers became thinner, thus improving the characteristics of the membranes; secondly, fiber distribution was narrower, resulting in more even distribution of properties throughout the materials. Raising the level of MAG concentration did not affect the circular morphology of the fibers, in agreement with the previous work by the authors.[21] This is a potential consequence of a slower electrospinning process caused by the high boiling point of the DMF solvent (153°C).

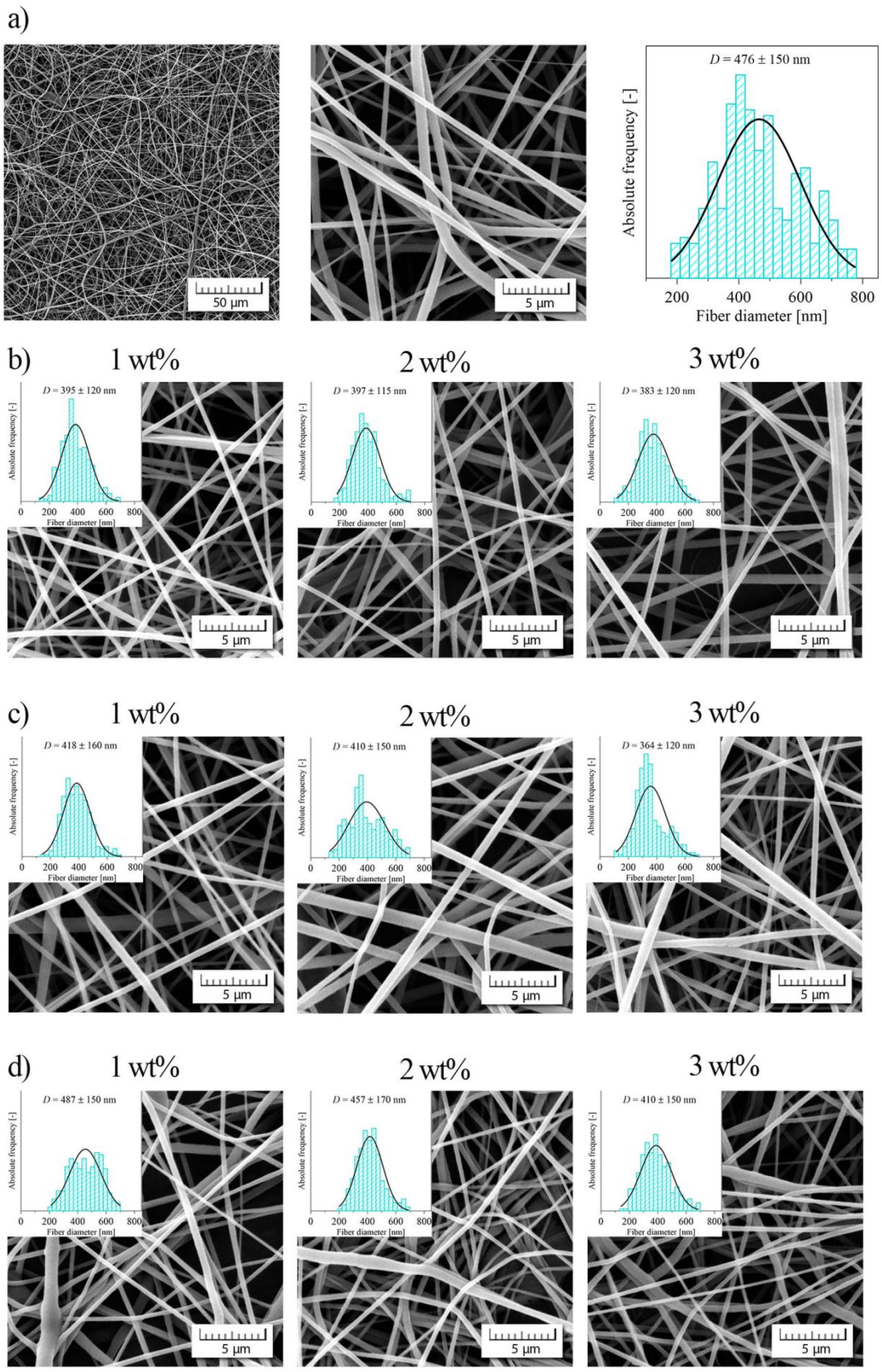
a)
50 µm
5 µm
D = 476 ± 150 nm
Absolute frequency [-]
200
400
600
800
Fiber diameter [nm]
b)
1 wt%
2 wt%
3 wt%
D = 395 ± 120 nm
D = 397 ± 115 nm
D = 383 ± 120 nm
c)
1 wt%
2 wt%
3 wt%
D = 418 ± 160 nm
D = 410 ± 150 nm
D = 364 ± 120 nm
d)
1 wt%
2 wt%
3 wt%
D = 487 ± 150 nm
D = 457 ± 170 nm
D = 410 ± 150 nm
5 µm

Figure 3. SEM images of the following nanofibers: a) neat PVDF-*co*-HFP; b) PVDF-*co*-HFP/MAG 8 (1-3 wt%); c) PVDF-*co*-HFP/MAG 10 (1-3 wt%); and d) PVDF-*co*-HFP/MAG 12 (1-3 wt%).

The mean values for fiber diameter and membrane pore size are key to determining the extent of water flux. This information for the final materials is presented in Table 2, which highlights a simultaneous decrease in both with respect to the contents of the MAG variants, as well as concurrent rise in the sequence from no MAG → MAG 8 → MAG 10 → MAG 12, wherein pore size reduced in parallel with a decrease in fiber diameter. The pore size distribution for all PVDF-*co*-HFP/MAG samples was narrower than for the neat PVDF-*co*-HFP membrane, as shown in Supplement Fig. S1.

Table 2. Mean nanofiber diameters and mean pore sizes of the membranes.

c [wt%]	Mean fiber diameter [nm]			Mean pore size [µm]		
	MAG 8	MAG 10	MAG 12	MAG 8	MAG 10	MAG 12
0	476±150^{a}			1.28±0.40^{ac}		
1	395±120^{b}	418±160^{b}	484±150^{a}	0.92±0.32^{b}	1.18±0.32^{ac}	1.40±0.40^{a}
2	397±115^{b}	410±150^{b}	457±170^{a}	0.90±0.35^{b}	1.05±0.34^{bc}	1.15±0.37^{bc}
3	383±120^{b}	364±120^{c}	410±150^{b}	0.84±0.26^{b}	0.86±0.26^{d}	1.05±0.31^{b}

The lower-case letters in the columns denote significant differences ($p<0.05$).

The surface properties of such membranes are crucial to their practical applicability. It is known that hydrophilic surfaces with minimum contact angles exhibit lower capillary pressure of the filtration media, thus enhancing the flow rate of water molecules through the membrane. The wettability of the membrane surfaces was characterized by measuring the water contact angle (WCA) by the static sessile drop method. Figure 4 lists mean values for WCA on the surfaces of the samples. As is evident, only a small amount of MAG (1 wt%) was capable of causing a remarkable drop in the contact angle from 127° for the neat PVDF-*co*-HFP to 25°, 13°, and 17° for MAG 8, MAG 10, and MAG 12, respectively. This abrupt change indicated that their hydrophilicity had been significantly enhanced through the introduction of polar hydroxyl head groups of the MAG molecular structure at the level of the surface.[39] The heightened hydrophilicity of the electrospun membranes instigated by the surfactants was confirmed by findings in the literature.[33,40] It is worthy of note that hydrophilic surfaces are beneficial in filtration applications as they can enhance the water permeability of the nanofibrous membranes.[35] This hydrophilic character of the membranes significantly boosts their associated antifouling properties[40], too, as proven herein through appropriate testing (see Subsections 3.2.3 and 3.2.4).

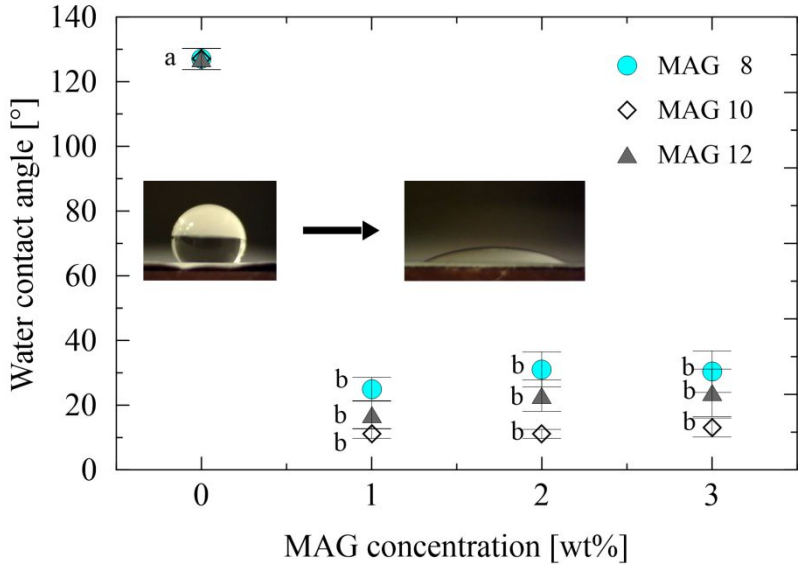

Figure 4. Wettability of samples of neat PVDF-*co*-HFP and PVDF-*co*-HFP modified with MAG. The lower-case letters denote significant differences ($p<0.05$) between specimens produced with one type of MAG at various concentrations and the neat PVDF-*co*-HFP membrane.

Figure 5 displays the FTIR-ATR spectra for the PVDF-*co*-HFP membranes with and without MAG 12. The spectrum for the neat PVDF-*co*-HFP (Fig. 5a) exhibits characteristic peaks for the PVDF material[41] at 834, 875, 1070, and 1400 cm^{-1} corresponding to $–CF_2$ and –CF bonds. The spectrum for MAG 12 (Fig. 5c) contains peaks typical of this structure, in agreement with the relevant literature[42], at 1730, 2950, and 2850 cm^{-1} pertaining to C=O and C-O stretching; in addition to a broad peak with its maximum at ca 3450 cm^{-1}, indicating O-H stretching of the hydroxyl groups due to the glycerol in the structure of the monolaurin.[43] In the case of the PVDF-*co*-HFP membrane enriched with MAG 12 (Fig. 5b), peaks appear at similar positions, with dominant ones at 1730 and 2950 cm^{-1}, revealing an interaction occurred between the PVDF polymer and monolaurin. The moderate rise in the intensity of these peaks reflects the greater extent of the MAG 12 functional group in PVDF-*co*-HFP (Supplement Fig. S2). A slight drop in the alpha phase (a peak at 763 cm^{-1}) is noticeable in the modified PVDF-*co*-HFP/MAG 12 sample, whereas the band at around 1275 cm^{-1} indicates a rise in β phase content (Supplement Fig. S3); the latter was also proven by calculations (Table 3).

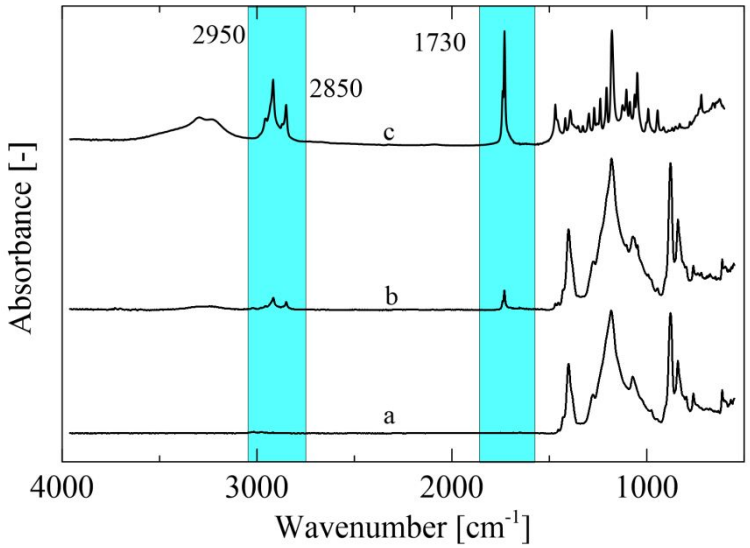

Figure 5. FTIR-ATR spectra for the following membranes: a) neat PVDF-*co*-HFP; b) PVDF-*co*-HFP modified with MAG 12 (2 wt%); and c) neat MAG 12.

XRD was performed to discern the phase composition of the electrospun PVDF-*co*-HFP and PVDF-*co*-HFP/MAG 12 membranes. The former of the two shows a moderately high peak at 17.5° and 18.4°, an intensive one at 20.3°, and the peak at 26.9° confirms the predominance of the crystalline α phase (Fig. 6); these correspond to reflections of 110, 100, 020, and 021.[42,44] In contrast, the XRD pattern for PVDF-*co*-HFP/MAG 12 (Fig. 6) presents a reflection peak at $2\theta = 20.7°$ of the β phase (200), which is dominant. In this case, the α phase recedes, as supported by the results of the FTIR analysis. Peaks are not visible for either sample at 35.9° (200) and 39.0° (211), unlike published findings for PVDF-*co*-HFP powder or electrospun PVDF-*co*-HFP membranes.[25]

Table 3. Phase content (wt%) of the electrospun fibers.

	PVDF-*co*-HFP	PVDF-*co*-HFP/MAG 12
β,γ phase	61.3	63.3
β phase	45.9	48.1
γ phase	58.2	59.8

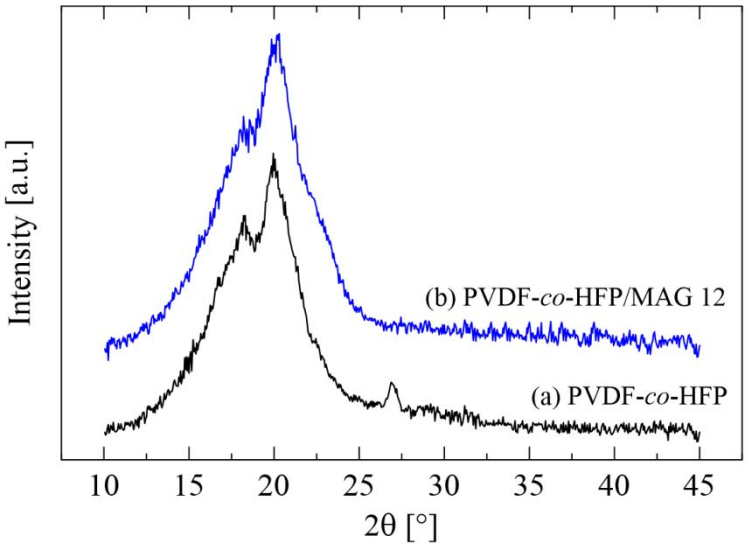

Figure 6. X-ray diffraction (XRD) patterns for the (a) PVDF-*co*-HFP and (b) PVDF-*co*-HFP/MAG 12 (2 wt%) electrospun membranes.

3.2.1. Water flux performance

The authors gauged the pure water flux of the membranes under transmembrane pressure (0.4 MPa) on a viscose, non-woven textile in combination with the prepared nanofibrous membrane (the latter at a set thickness of 30 ± 3 μm). In general, permeability is dependent on the pore and fiber sizes, thicknesses, and wettability of the membrane.[44,45] All the modified samples demonstrated a water permeation flux that was at least six times higher than that of the neat PVDF-*co*-HFP nanofibrous membranes (see Fig. 7). In this instance, it would seem that pore and fiber sizes merely exerted a minor effect compared to the dramatically improved wettability. Adding a small amount of the surfactant to the electrospun polymeric solution significantly increased the filtration performance of the nanofibrous membranes. The PVDF-*co*-HFP/MAG nanofibrous membranes exhibited similar extents of water flux performance (at the same pressure – 0.4 MPa) to the sample with the multi-arm, amphiphilic, fluxible poly(*p*-phenylene terephthalamide) (f-PPTA) addition in neat PVDF[18], except when f-PPTA represented 20 wt% of the additive. In this case, 1 wt% of MAG was sufficient to raise water flux performance to the same level.

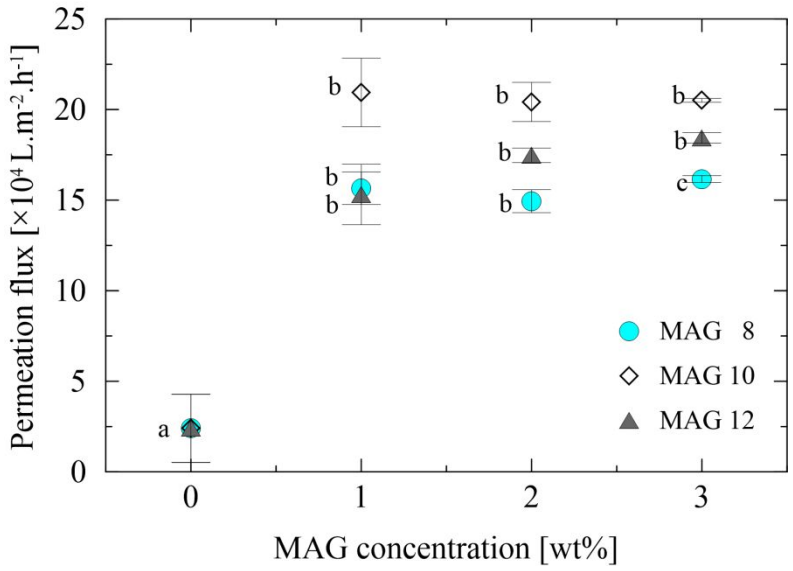

Figure 7. Permeation fluxes of the neat PVDF-*co*-HFP and PVDF-*co*-HFP membranes modified with MAG. The lower-case letters denote significant differences ($p<0.05$) between the specimens produced with one type of MAG at various concentrations and the neat PVDF-*co*-HFP membrane.

3.2.2. Antibacterial activity

Agar diffusion tests were first carried out for the pure MAG samples. Previous research has reported MAG to be effective against Gram-positive and Gram-negative bacteria, yeasts, and molds.[46-48] As detailed in Table 4, all the MAG variants demonstrated inhibition against Gram-positive *Staphylococcus aureus*, the most effective being MAG 12. Notably, only MAG 10 acted against gram-negative *Escherichia coli*.

The neat PVDF-*co*-HFP nanofibrous membrane was applied as the control to contrast with the membranes containing MAG. While adding 1 wt% of MAG 12 resulted in just a slight increase of inhibitory activity, the concentration of 2 wt% inhibited *S. aureus* more significantly, with no considerable change manifested through raising MAG concentration further (Table 4).

Table 4. Agar disk diffusion testing of 5 wt% MAG variants in ethanol and PVDF-*co*-HFP membranes against *S. aureus* and *E. coli* (9 mm pieces of paper or PVDF-*co*-HFP disks).

Inhibition zone (mm)	*Staphylococcus aureus*	*Escherichia coli*
MAG 8	13*	N
MAG 10	15	12
MAG 12	26	N
PVDF-*co*-HFP	N	N
PVDF-*co*-HFP/1 wt% MAG 12	10	N
PVDF-*co*-HFP/2 wt % MAG 12	18	N

PVDF-*co*-HFP/3 wt % MAG 12	17	N

*The number represents the diameter of the inhibition zone including the 9 mm piece of paper/ PVDF-*co*-HFP disk. N – no inhibition zone observed.

The agar diffusion test was also conducted on the PVDF-*co*-HFP and PVDF-*co*-HFP/MAG nanofibrous membranes after the filtration experiment. Antibacterial activity occurred against Gram-positive *S. aureus* in samples containing 2 wt% MAG 12 and higher. No inhibition zone was generated by MAG 8 and MAG 10. Hence, it can be supposed that the MAG variants with shorter carbon chains were either unable to diffuse from the nanofibers sufficiently and prevent microbial growth, or the effect exerted was weaker than described in the literature.[20,49,50] Both of the bacterial strains actually grew under the PVDF-*co*-HFP nanofibrous membranes, while no inhibition zones on the agar plates against *E. coli* were observed in this study. Such growth did not take place under the tested PVDF-*co*-HFP/MAG disks, though. Similarly, there was no activity of monolaurin (MAG 12) against *E. coli*, in contrast with *S. aureus* in the time-kill assay.[43] The nanofibrous membrane PVDF-*co*-HFP/MAG 12 exhibited good antibacterial activity against *S. aureus* even after the filtration test; interestingly, its activity was not diminished (Table 5, Supplement Fig. S4), instead it demonstrated higher efficacy than before filtration.

Table 5. Agar disk diffusion testing of PVDF-*co*-HFP and PVDF-*co*-HFP/MAG membranes before and after filtration against *Staphylococcus aureus* (25 mm PVDF-*co*-HFP membrane disks).

Inhibition zone (mm)	Before filtration	After filtration (mL)		
		100	500	1000
PVDF-*co*-HFP	N*	N	N	N
PVDF-*co*-HFP/1-3 wt% MAG 8;10	N	N	N	N
PVDF-*co*-HFP/1 wt% MAG 12	26	27	N	N
PVDF-*co*-HFP/2 wt% MAG 12	27	32	N	N
PVDF-*co*-HFP/3 wt% MAG 12	26	30	26	29

*N – no inhibition zone observed.

The antibacterial activity against *S. aureus* and *E. coli* of the PVDF-*co*-HFP membranes was investigated by a standard flask shaking method (Table 6). Modifying the PVDF-*co*-HFP nanofibrous membranes by supplementing them with MAG 12 significantly reduced the number of bacteria present by up to 97.11% (*E. coli*) and even 99.99% (*S. aureus*) after 1440 minutes. Although these measured values are very high, greater efficacy has been reported for samples based on PVDF/PVA modified by $AgNO_3$ in the literature.[25]

In this study, *S. aureus* proved highly susceptible to this modification of the membrane after just 60 minutes, according to the disk diffusion test results (Tables 4 and 5). A similar susceptibility has been reported by other authors against *S. aureus* by PVDF nanofibrous membranes modified with quaternary ammonium compounds[51] and shellac nanofibers[29]

modified by monolaurin (MAG 12). Such trend was not exerted herein against *E. coli,* though, where it took up to 1440 minutes for a significant level of decrease to occur compared to the neat PVDF-*co*-FHP membrane (Table 6).

Table 6. Rate of reduction in percent (R%) of *S. aureus* and *E. coli* over time (60, 120, 300, 1440 min.) through direct contact with the nanofibrous membranes with or without the active antibacterial compound (MAG 12) in relation to the control material (aluminum foil without nanofibers).

	Staphylococcus aureus			
	60	**120**	**300**	**1440**
PVDF-*co*-HFP	28.37^{aA}	38.85^{aB}	85.61^{aC}	99.90^{aD}
PVDF-*co*-HFP/2 wt% MAG 12	36.46^{bA}	88.17^{bB}	76.73^{bC}	99.99^{aD}
	Escherichia coli			
	60	**120**	**300**	**1440**
PVDF-*co*-HFP	46.52^{aA}	50.01^{aB}	56.62^{aC}	64.47^{aD}
PVDF-*co*-HFP/2 wt% MAG 12	45.25^{aA}	42.84^{bB}	50.64^{bC}	97.11^{bD}

The lower-case and upper-case letters in the fields denote significant differences ($p<0.05$).

The antibacterial activity of the PVDF-*co*-HFP and PVDF-*co*-HFP/MAG 12 nanofibrous membranes was gauged by the contact method according to ISO 22196:2011 against *S. aureus* and *E. coli*. The counts of recovered viable bacteria were determined and the tests were found to be valid. The reduction in viable cell numbers was calculated as R = 0.9 for *S. aureus* and R = 1.4 for *E. coli*. Bacteria on the PVDF-*co*-HFP/MAG nanofibers reduced in quantity by about one or more logarithmic order. Even though *S. aureus* was susceptible to the MAG 12 incorporated in the PVDF-*co*-HFP membrane in comparison with the *E. coli* cells (Tables 4 and 5), the value for R was higher for *E. coli.* This suggests that the inhibition mechanism was not solely associated with the active compound (MAG 12) but other factors were also involved. The assumption is that it pertained to the major shift in the hydrophobic character of the nanofibers, as evidenced by the change in water contact angle (Fig. 4) and the surface charges of the bacteria (*S. aureus* and *E. coli*).[52,53] In terms of staphylococci, the initial interaction between the cells and surface is facilitated by the lipid moiety of lipoteichoic acid, which allows the bacterium to overcome the natural electrostatic repulsion of the surface.[54]

The antibacterial experiment proved that the MAG 12 incorporated in the nanofibrous membrane significantly inhibited the growth of *S. aureus* bacteria, whereas less activity was observed against *E. coli* in the diffusion test.

3.2.3 Antifouling activity

Developing membranes with antibacterial surfaces is an interesting solution to water filtration, as they have the capacity to inhibit bacterial attachment and proliferation on the

surfaces of materials and prevent biofilm formation. Bacterial attachment is induced by hydrophobic and electrokinetic interactions with surfaces.[55] Highly hydrophobic cells adhere strongly to hydrophobic materials, while hydrophilic cells show the same affinity for hydrophilic surfaces.[56] In this study, both bacterial strains adhered to the neat PVDF-*co*-HFP membrane, although this adherence was significantly reduced in the presence of the MAG 12 additive. The MAG membranes significantly inhibited biofouling by the Gram-positive and Gram-negative bacteria (Fig. 8). The count of sessile *S. aureus* cells that remained adhered to PVDF-*co*-HFP/MAG 12 after 72 hours was 100 times (2 logarithmic orders) lower than for the control material (aluminum foil). *E. coli* showed resistance in this respect, though the count was still less than for the neat membrane, which is a consequence of the difference in cell wall structure with more lipids and its particular hydrophilic properties. This was also evidenced by fluorescence and electron microscopy (SEM), where biofilm production was prevented on PVDF-*co*-HFP/MAG 12 (Figs. 9 and 10).

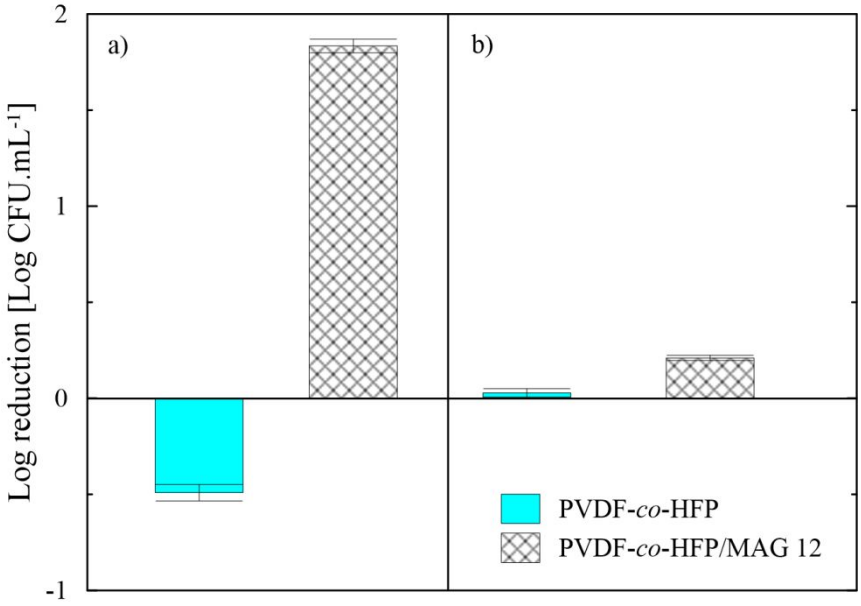

Figure 8. Logarithmic reduction (Log CFU.mL^{-1}) as an expression of adhesion (antifouling activity) by a) *Staphylococcus aureus* and, b) *Escherichia coli* to the PVDF-*co*-HFP and PVDF-*co*-HFP/2 wt% MAG 12 nanofibrous membranes, in relation to the control material (aluminum foil).

3.2.4. Biofilm formation test – SEM and fluorescence microscopy

It is known that an antifouling effect is associated with the cell size, morphology, shape, and hydrophilicity of a substrate.[57] In this context, two independent experiments to observe biofilm formation were carried out on PVDF-*co*-HFP (as the control) and PVDF-*co*-HFP/MAG 12. The attachment and adhesion of cells to the nanofibrous systems were evaluated. The colonization of surface bacteria results from the processes inducing a change in the behavior and interaction of microbial cells with the present substrate.[37]

LIVE/DEAD bacterial viability assays were performed, and fluorescence microscopy was applied to verify the ability of both bacteria to form biofilm on PVDF-*co*-HFP and PVDF-*co*-HFP/MAG 12 nanofibers (Figs. 9 and 10). In these images, the nanofibers are shown as green, and numerous live bacterial cells (*S. aureus and E. coli*, stained green) were observed on the PVDF-*co*-HFP nanofibers (Figs. 9a and 10a, fluorescence microscopy). According to the results, the unmodified PVDF-*co*-HFP membrane showed neither antibacterial nor antifouling properties, only a few dead bacterial cells (red cells) were visible on the PVDF-*co*-HFP nanofibers; this may be considered a normal bacterial life cycle after 72 hours of cultivation. Supported by SEM (Figs. 9a and 10a) it can be concluded that *S. aureus and E. coli* were able to form biofilm on the neat membrane. In terms of *S. aureus*, the cells were entangled in the fibers, whereas *E. coli* was unable to penetrate the fibrous structure due to the cell size and rod morphology. The tendency of both bacteria to form a biofilm on the PVDF-*co*-HFP membranes was observed. A neat PVDF membrane has been reported earlier as not affecting bacterial response.[25] Circumstances exist, in fact, where the ability to form biofilm is useful, such as in agriculture (nutrient supply and controlling plant diseases) and the environment (bioremediation of polluted soils and wastewater).[58]

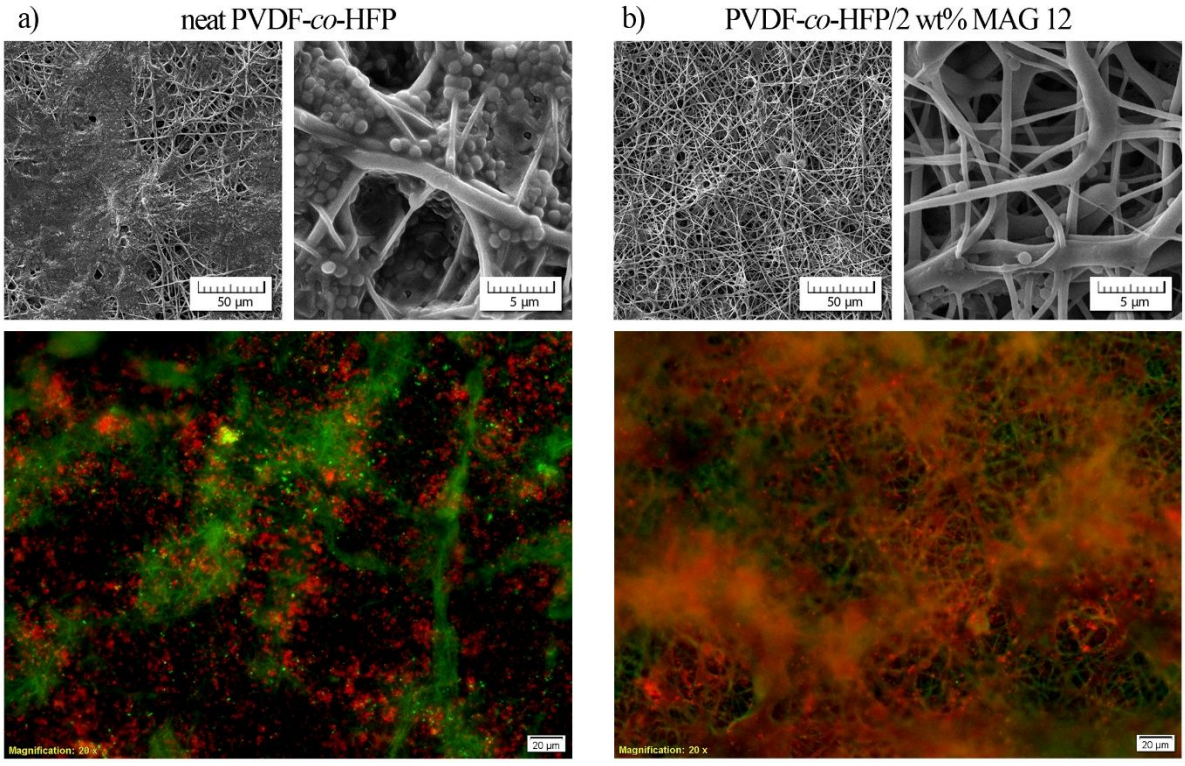

Figure 9. SEM and fluorescence microscopy of the a) PVDF-*co*-HFP and b) PVDF-*co*-HFP/2 wt% MAG 12 nanofibrous membranes after 72 h cultivation with *Staphylococcus aureus*.

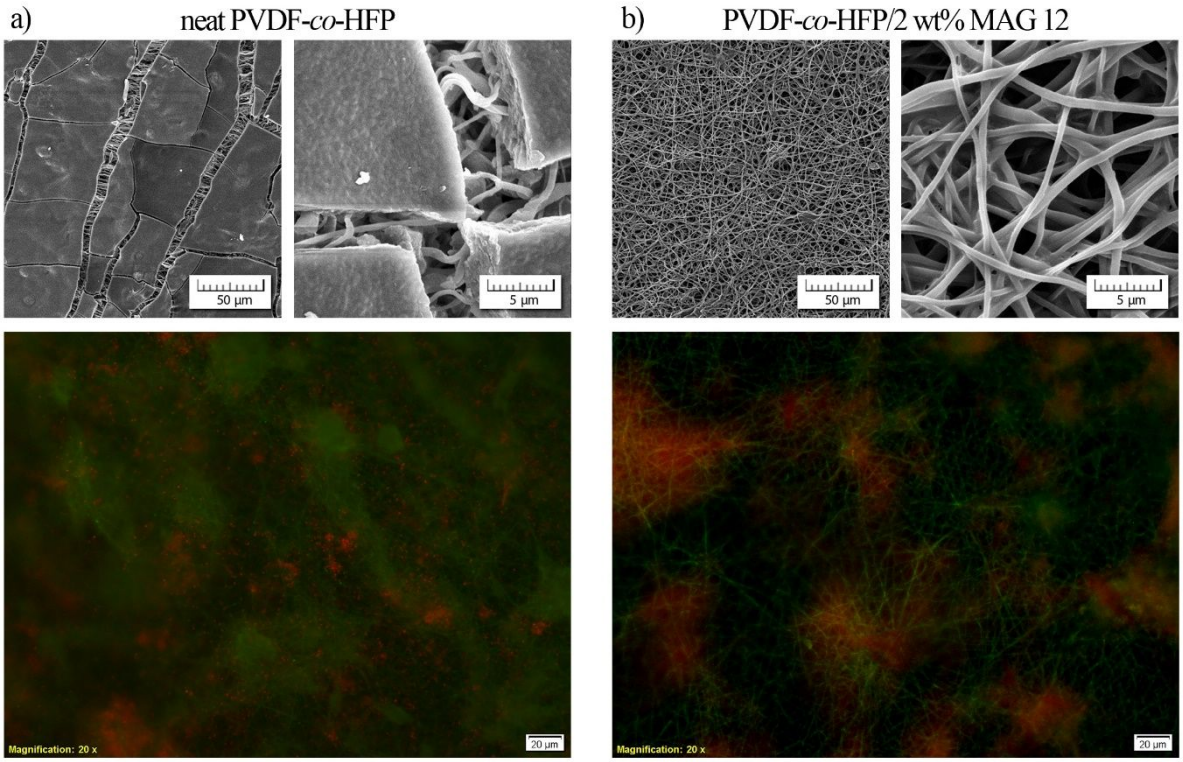

Figure 10. SEM and fluorescence microscopy of the a) PVDF-*co*-HFP and b) PVDF-*co*-HFP/2 wt% MAG 12 nanofibrous membranes after 72 h cultivation with *Escherichia coli.*

In contrast, the surface images for PVDF-*co*-HFP/2 wt% MAG 12 after 72 h of bacterial growth reveal no presence of biofilm (Figs. 9b and 10b). No bacterial cells (*S. aureus, E. coli*) were observed either by fluorescence microscopy or SEM. If present at all, they were stained red, indicating they were dead (Figs. 9b and 10b, fluorescence microscopy). The PVDF-*co*-HFP/MAG 12 membrane exhibited both antimicrobial and antifouling effects (Tabs. 5 and 6, Fig. 8). By combining all of the applied methods, the antibacterial activity of MAG 12 (2 wt%) against *S. aureus* was validated. Staphylococci were entrapped in the nanofibrous structure enriched with MAG 12; hence, biofilm could not be formed by them as they were killed through direct contact. The results of the fluorescence microscopy unambiguously prove that the prepared material does not permit biofilm formation due to low bacterial adhesion, as described earlier in the section on antifouling activity (Subsection 3.2.3.). As MAG is antibacterial and generally considered safe for foodstuffs, incorporating MAG 12 into PVDF-*co*-HFP shows excellent potential for widespread use in the food industry[56] and water treatment[16] due to its capacity to prevent the build-up of biofilm.

4. Discussion

It is well-known that an increase (decrease) in viscosity reflects in the increasing (decreasing) of nanofiber diameters[59] and hence, it participates in the efficiency of nanofibrous membranes. As supposed, rheological measurements proved strong interlacing between shear viscosity (Fig. 2) and fiber morphology (Fig 3). Practically identical values of shear viscosity for the neat copolymer and PVDF-*co*-HFP/1 wt% MAG 12 resulted in nearly

identical mean nanofiber diameters 476 and 484 nm. Analogously the highest decrease in viscosity with weighted concentrations exhibited by MAG 12 is reflected in a consecutive decrease in mean diameter of respective nanofibers (484↘457↘410 nm). Adequate behavior is also possible to document for MAG 10. Nanofibers containing MAG 8 exhibited pronounced monomodal fiber diameter distribution with no tendencies towards partially bimodal representation in comparison with nanofibers containing MAG 10 and MAG 12 as documented in Fig. 3. This reflects in the morphology of nanofibrous mats (Fig. 3) with apparently even distribution of equivalent nanofibers for MAG 8 for which the mean fiber diameter is mostly invariant with respect to MAG 8 participation and a decrease of the mean pore size with increasing participation is only moderate, see Table 2.

Moderate decrease in viscosity, conductivity, surface tension and fiber diameter with increasing MAG concentrations regardless of the specific type is documented in Tables 1 and 2, and Fig. 2. Monoacylglycerols belong to non-ionic surfactants, which have no electrical net charge on the polar head group, and form relatively stable large micellar aggregates after the critical micelle concentration is achieved. However, contrary to ionic surface active agents, these non-ionic structures do not bind cooperatively to the polymer substrate at the critical aggregation concentration.

A higher water permeate flux is always required for better membrane filtration performance. Therefore the fiber diameter, pore size and wettability are key parameters for investigating the filtration properties. In this case, the modified membranes exhibit not only lower fiber diameter and pore size but dramatic enhancement in wettability which influences pure water flux. An increased filtration performance from 2.404 to 20.507×10^4 $L.m^{-2}.h^{-1}$ was proved due to the interaction of amphiphilic MAG molecules with PVDF-*co*-HFP hydrophobic chains, increasing the affinity toward water molecules and facilitating the water permeation flux as depicted in Fig. 7. This fact correlates with the results of water contact angle measurement revealing the drop of almost 90 % in the case of MAG 10.

The change of the PVDF-*co*-HFP crystalline structure by MAG proves the excellent compatibility between polymer chains and surfactant. The results from the XRD measurements indicate that the addition of MAG 12 favors the formation of β-crystals. Therefore, the β phase is dominated in electrospun PVDF-*co*-HFP/MAG 12. This indication is confirmed in Table 3. The β-phase has the highest dipole moment per unit cell compared to the alpha and epsilon phases which have no electrical activity because the packing of their dipole moment is antiparallel within the unit cell. The β-phase present in PVDF-*co*-HFP and especially in PVDF-*co*-HFP/MAG 12 might hold an advantage over other polymers used in manufacturing fibrous filters due to its additional contribution as an excellent electret.[60]

The excellent compatibility of safety and antibacterial MAGs with PVDF-*co*-HFP avoids the problems of being easily washed away during the filtration performance. In addition, the greatly improved antibacterial activity and antifouling ability is very helpful in the long life extension separation membrane. The mechanism of MAGs antimicrobial activity is not precisely known, although within the disintegration of plasma membrane by fatty acids belongs among the most discussed possibilities.[61] They are more active against Gram-positive bacteria because of their polysaccharide cell wall, and less active against Gram-negative

bacteria having lipopolysaccharides.[62] This claim was confirmed by the presented results in Tables 4 and 5. A modified nanofibrous membrane PVDF-*co*-HFP/MAG 12 shows significant antibacterial activity against *S. aureus* even after the filtration performance, whereas lower activity was observed against *E. coli* in the diffusion test. From the antifouling tests results that the addition of MAG in membrane inhibited the biofouling by Gram-positive and Gram-negative bacteria (Fig. 8). Substantially improved surface hydrophilicity by MAG 12 addition (Fig. 4) effectively reduces the interaction force between membrane surface and cells proved also by increased water flux permeation (Fig. 7). The improvement of bacteria fouling resistance may be likely attributed to the hydration interaction between water molecules and hydrophilic hydroxyl head groups in the MAG molecular structure resulting in a repulsive force of membrane surface to bacteria.[63]

5. Conclusions

The electrospinning method was used to manufacture novel PVDF-co-HFP/MAG nanofibrous membranes with a high wettability and antibacterial properties. The effects of the various types of MAGs and their concentration on electrospun membranes were investigated. The results showed that the addition of a small amount (1 wt%) of non-ionic surfactant improved the electrospinnability and the surface properties of the produced membranes by enhancing their hydrophilicity and permeability. Besides, monolaurin MAG 12 is the unique antibacterial agent enabling an increase in antibacterial activity against Gram-positive bacteria. Moreover, the modified membrane exhibited excellent antifouling ability compared to the neat PVDF-co-HFP one. This study provides a simple, environmentally friendly approach for the preparation of highly efficient antibacterial membranes. For these reasons, the functionalized PVDF-co-HFP/MAG 12 nanofibrous membrane is a potential candidate for antifouling filtration membrane to wastewater treatment.

Acknowledgments

The authors (P. Peer, P. F., and J. Z.) acknowledge the support lent by the program INTER-EXCELLENCE, a subprogram of INTER-COST by the Ministry of Education, Youth and Sports CR, grant No. LTC19034. Institutional assistance was provided by the Czech Academy of Sciences, Czech Republic (RVO: 67985874). The authors (M. J., J. S. and P. Pleva) acknowledges the support given by TACR, project No. TJ04000226, and the author (A. O. S.) is grateful to the project VEGA 2/0168/21 and APVV 18-0420.

Supporting Information

The Figures providing the following supporting information are introduced:

- The pore size distribution of the neat PVDF-co-HFP and MAG (8, 10, 12) modified (1, 2, 3 wt%) membranes.

- The FTIR-ATR spectra of the PVDF-co-HFP/MAG 12 (1, 2, 3 wt%) membranes.

- The details of FTIR-ATR spectra of the neat PVDF-co-HFP and modified with MAG 12 (2 wt%) membranes.

- The agar diffusion test of PVDF-co-HFP/3 wt% MAG 12 nanofibrous membrane after filtration of distilled water.

References

(1) Kang, G. D.; Cao, Y. M. Application and modification of poly(vinylidene fluoride) (PVDF) membranes - A review. *J. Membr. Sci*. **2014**, *463*, 145–165.

(2) Zhu, Y.; Wang, D.; Jiang, L.; Jin, J. Recent progress in developing advanced membranes for emulsified oil/water separation. *NPG Asia Mater.* **2014**, *6*, e101.

(3) Lalia, B.S.; Guillen-Burrieza, E.; Arafat, H.A.; Hashaikeh, R. Fabrication and characterization of polyvinylidenefluoride-co-hexafluoropropylene (PVDF-HFP) electrospun membranes for direct contact membrane distillation. *J. Membr. Sci.* **2013**, *428*, 104–115.

(4) Wang, J.; Ma, M.; Yang, J.; Chen, L.; Yu, P.; Wang, J.; Gong. D.; Deng, S.; Wen, X.; Zeng, Z. In vitro antibacterial activity and mechanism of monocaprylin against *Escherichia coli* and *Staphylococcus aureus*. *J. Food Prot.* **2018**, *8*1, 1988–1996.

(5) Chen, Y.; Qiu, L.; Ma, X.; Chu, Z.; Zhuang, Z.; Dong, L.; Du, P.; Xiong, J. Electrospun PMIA and PVDF-HFP composite nanofibrous membranes with two different structures for improved lithium-ion battery separators. *Solid State Ion*. **2020**, *347*, 115253.

(6) Liu, X.; Lin, T.; Fang, J.; Yao, G.; Zhao, H.; Dodson, M.; Wang, X. In Vivo wound healing and antibacterial performances of electrospun nanofibre membranes. *J. Biomed. Mater. Res. Part A* **2010**, *94A*, 499–508.

(7) Ganesh, V. A; Kundukad, B.; Cheng, D.; Radhakrishnan, S.; Ramakrishna, S.; Van Vliet, K. J. Engineering silver-zwitterionic composite nanofiber membrane for bacterial fouling resistance. *J. Appl. Polym. Sci.* **2019**, *136*, 47580.

(8) Spasova, M.; Manolova, N.; Markova N.; Rashkov, I. Superhydrophobic PVDF and PVDF-HFP nanofibrous mats with antibacterial and anti-biofouling properties. *Appl. Surf. Sci.* **2016**, *363*, 363–371.

(9) Spasova, M.; Manolova, N.; Markova N.; Rashkov, I. Tuning the properties of PVDF or PVDF-HFP fibrous materials decorated with ZnO nanoparticles by applying electrospinning alone or in conjunction with electrospraying. *Fiber. Polym*. **2017**, *18*, 649–657.

(10) Li, X.; Qing, W.; Wu, Y.; Shao, S.; Peng, L. E.; Yang, Y.; Wang, P.; Liu, F.; Tang, C. Y. Omniphobic nanofibrous membrane with pine-needle-like hierarchical nanostructures: toward enhanced performance for membrane distillation. *ACS Appl. Mater. Interfaces* **2019**, *11*, 47963–47971.

(11) Liu, Z.; Qin, D.; Zhao, J.; Feng, Q.; Li, Z.; Bai, H.; Sun, D. D. Efficient oil/water separation membrane derived from super-flexible and superhydrophilic core-shell organic/inorganic nanofibrous architectures. *Polymers* **2019**, *11*, 974.

(12) Rodríguez-Tobías, H.; Morales, G.; Grande, D. Comprehensive review on electrospinning techniques as versatile approaches toward antimicrobial biopolymeric composite fibers. *Mater. Sci. Eng. C-Mater. Biol. Appl*. **2019**, *101*, 306–322.

(13) Kurtz, I. S.; Schiffman, J. D. Current and emerging approaches to engineer antibacterial and antifouling electrospun nanofibers. *Materials* **2018**, *11*, 1059.

(14) Simões, D.; Miguel, S.P.; Ribeiro, M.P.; Coutinho, P.; Mendonça, A.G.; Correia, I.J. Recent advances on antimicrobial wound dressing: A review. *Eur. J. Pharm. Biopharm*. **2018**, *127*, 130–141.

(15) Graça, M. F. P.; de Melo-Diogo, D.; Correia, I. J.; Moreira, A. F. Electrospun asymmetric membranes as promising wound dressings: A review. *Pharmaceutics* **2021**, *13*, 183.

(16) García A.; Rodríguez, B.; Giraldo, H.; Quintero, Y.; Quezada, R.; Hassan, N.; Estay, H. Copper-modified polymeric membranes for water treatment: A comprehensive review. *Membranes* **2021**, *11*, 93.

(17) Brayner, R.; Ferrari-Iliou, R.; Brivois, N.; Djediat, S.; Benedetti, M. F.; Fiévet, F. Toxicological impact studies based on *Escherichia coli* bacteria in ultrafine ZnO nanoparticles colloidal medium. *Nano Lett.* **2006**, *6*, 866–870.

(18) Chen, Z.; Du, X.-A.; Liu, Y.; Ju, Y.; Song, S.; Dong, L. A high-efficiency ultrafiltration nanofibrous membrane with remarkable antifouling and antibacterial ability. *J. Mater. Chem. A* **2018**, *6*, 15191–15199.

(19) Kabara, J. J.; Swieczkowski, D. M.; Conley, A. J.; Truant, J. P. Fatty acids and derivatives as antimicrobial agents. *Antimicrob. Agents Chemother*. **1972**, *2*, 23–28.

(20) Yoon, B. K.; Jackman, J. A.; Valle-Gonzalez, E. R.; Cho, N.-J. Antibacterial free fatty acids and monoglycerides: Biological activities, experimental testing, and therapeutic applications. *Int. J. Mol. Sci.* **2018**, *19*, 1114.

(21) Peer, P.; Sedlarikova, J.; Janalikova, M.; Kucerova, L.; Pleva, P. Novel polyvinyl butyral/monoacylglycerol nanofibrous membrane with antifouling activity. *Materials* **2020**, *13*, 3662.

(22) Janis, R.; Klasek, A.; Krejci, J.; Bobalova, J. Influence of some chromium complexes on the conversion rate of glycidol—Fatty acid reaction. *Tenside Surfactants Deterg*. **2005**, *42*, 44–48.

(23) Castkova, K.; Kastyl, J.; Sobola, D.; Petrus, J.; Stastna, E.; Riha, D.; Tofel, P. Structure-properties relationship of electrospun PVDF fibers. *Nanomaterials* **2020**, *10*, 1221.

(24) CLSI, Performance Standards for Antimicrobial Disk Susceptibility Tests, Approved Standard, 7th ed., CLSI document M02-A11. Clinical and Laboratory Standards Institute, 950 West Valley Road, Suite 2500, Wayne, Pennsylvania 19087, USA, 2012.

(25) Coelho, D.; Sampaio, A.; Silva, C. J. S. M.; Felgueras, H. P.; Amorim, M. T. P.; Zille, A. Antibacterial electrospun poly(vinyl alcohol)/enzymatic synthesized poly(catechol) nanofibrous midlayer membrane for ultrafiltration. *ACS Appl. Mater. Interfaces* **2017**, *9*, 33107–33118.

(26) ISO 22196 (2011). "Measurement of Antibacterial Activity on Plastics and Other Non-Porous Surfaces," International Organization for Standardization, Geneva, Switzerland.

(27) Rosen, M. J.; Kunjappu, J. T. Surfactants and Interfacial Phenomena; John Wiley & Sons: 2012; Chapter 1, pp 1−3.

(28) Molecular Probes, Invitrogen detection technologies [online]. Molecular Probes, Inc. Available at: https://assets.thermofisher.com/TFS-Assets/LSG/manuals/mp07007.pdf.

(29) Wang, H.; Xie, H.; Wang, S.; Gao, Z.; Li, C.; Hu, G. H.; Xiong, C. Enhanced dielectric property and energy storage density of PVDF-HFP based dielectric composites by incorporation of silver nanoparticles-decorated exfoliated montmorillnonite nanoplatelets. *Compos. Part A Appl. Sci. Manuf.* **2018**, *108*, 62–68.

(30) Zaidouny, L.; Abou-Daher, M.; Tehrani-Bagha, A. R.; Ghali, K.; Ghaddar, N. Electrospun nanofibrous polyvinylidene fluoride-co-hexafluoropropylene membranes for oil-water separation *J. Appl. Polym. Sci*. **2020**, *137*, e49394.

(31) Peer, P.; Zelenkova, J.; Filip, P. An estimate of the onset of beadless character of electrospun nanofibres using rheological characterization. *Polymers* **2021**, *13*, 256.

(32) Essalhi, M.; Khayet, M. Self-sustained webs of polyvinylidene fluoride electrospun nano-fibers: Effects of polymer concentration and desalination by direct contact membrane distillation. *J. Membr. Sci*. **2014**, *454*, 133–143.

(33) Beigmoradi, R.; Samimi, A.; Mohebbi-Kalhori, D. Fabrication of polymeric nanofibrous mats with controllable structure and enhanced wetting behavior using one-step electrospinning. *Polymer* **2018**, *143*, 271–280.

(34) Mohammad, A. A., Alkhaldi, K., Al-Tuwaim, M. S.; Al-Jimaz, A. S. Viscosity and surface tension of binary systems of N,N-dimethylformamide with alkan-1-ols at different temperatures. *J. Chem. Thermodyn*. **2013**, *56*, 106–113.

(35) Park, J., Kim, S. Preparation and characterization of antimicrobial electrospun poly(vinyl alcohol) nanofibers containing benzyl triethylammonium chloride. *React. Funct. Polym.* **2015**, *93*, 30–37.

(36) Rosic, R.; Pelipenko, J.; Kristl, J.; Kocbek, P.; Bester-Rogac, M.; Baumgartner, S. Physical characteristics of poly (vinyl alcohol) solutions in relation to electrospun nanofiber formation. *Eur. Polym. J.* **2013**, *49*, 290–298.

(37) Fang, W.; Yang, S.; Yuan, T. Q.; Charlton, A.; Sun, R. C. Effects of various surfactants on alkali lignin electrospinning ability and spun fibers. *Ind. Eng. Chem. Research* **2017**, *56*, 9551–9559.

(38) Talwar, S.; Krishnan, A. S.; Hinestroza, J. P.; Pourdeyhimi, B.; Khan, S. A. Electrospun nanofibers with associative polymer-surfactant systems. *Macromolecules* **2010**, *43*, 7650–7656.

(39) Jung, Y. H.; Kim, H. Y.; Lee, D. R.; Park, S. Y. Characterization of PVOH nonwoven mats prepared from surfactant-polymer system via electrospinning. *Macromol. Res*. **2005**, *13*, 385–390.

(40) Saraswathi, M.; Rana, D.; Divya, K. Versatility of hydrophilic and antifouling PVDF ultrafiltration membranes tailored with polyhexanide coated copper oxide nanoparticles. *Polym. Test.* **2020**, *84*, 106367.

(41) Saini, B.; Vaghani, D.; Khuntia, S.; Sinha, M. K.; Patel, A.; Pindoria, R. A novel stimuli-response and fouling resistant PVDF ultrafiltration membrane prepared by using amphiphilic copolymer of poly(vinylidene fluoride) and poly(2-N-morpholino)ethyl methacrylate. *J. Membr. Sci*. **2020**, *603*, 118047.

(42) Sadiq, S.; Imran, M.; Habib, H.; Shabbir, S.; Ihasn, A.; Zafar, Y.; Hafeez, F. Y. Potential of monolaurin based food-grade nano-micelles loaded with nisin Z for synergistic antimicrobial action against *Staphylococcus aureus*. *LWT-Food Sci. Tech*. **2016**, *71*, 227–233.

(43) Chinatangkul, N.; Limmatvapirat, C.; Nunthanid, J.; Luangtana-Anan, M.; Sriamornsak, P.; Limmatvapirat, S. Design and characterization of monolaurin loaded electrospun shellac nanofibers with antimicrobial activity. *Asian J. Pharm. Sci.* **2018**, *13*, 459–471.

(44) Zhong, S.; Zhang, Y.; Lim, C. T. Fabrication of large pores in electrospun nanofibrous scaffolds for cellular infiltration: a review. *Tissue Eng. B Rev.* **2011**, *18*, 77–87.

(45) Z. Wang, Z.; Crandall, C.; Sahadevan, R.; Menkhaus, T. J.; Fong, H. Microfiltration performance of electrospun nanofiber membranes with varied fiber diameters and different membrane porosities and thicknesses. *Polymer* **2017**, *114*, 64–72.

(46) Preuss, H. G.; Echard, B.; Enig, M.; Brook, I.; Elliott, T. B. Minimum inhibitory concentrations of herbal essential oils and monolaurin for gram-positive and gram-negative bacteria. *Mol. Cell. Biochem*. **2005**, *272*, 29–34

(47) Altieri, C.; Bevilacqua, A.; Cardillo, D.; Sinigaglia, M. Effectiveness of fatty acids and their monoglycerides against gram-negative pathogens. *Int. J. Food Sci. Technol.* **2009**, *44*, 359–366.

(48) Bunkova, L.; Krejci, J.; Janis, R.; Kasparkova, V.; Vltavska, P.; Kulendova, L.; Bunka, F. Influence of monoacylglycerols on growth inhibition of micromycetes in vitro and on bread. *Eur. J. Lipid Sci. Technol*. **2010**, *112*, 173–179.

(49) Sevcikova, P.; Kasparkova, V.; Hauerlandova, I.; Humpolicek, P.; Kucekova, Z.; Bunkova, L. Formulation, antibacterial activity, and cytotoxicity of 1-monoacylglycerol microemulsions. *Eur. J. Lipid Sci. Technol*. **2014**, *116*, 448–457.

(50) Hauerlandova, I.; Lorencova, E.; Bunka, F.; Navratil, J.; Janeckova, K.; Bunkova, L. The influence of fat and monoacylglycerols on growth of spore-forming bacteria in processed cheese. *Int. J. Food Microbiol*. **2014**, *182*, 37–43.

(51) Park, J. A.; Cho, K. Y.; Han, C. H.; Nam, A.; Kim, J. H.; Lee, S. H.; Choi, J. W. Quaternized amphiphilic block copolymers/graphene oxide and a poly(vinyl alcohol) coating layer on graphene oxide/poly(vinylidene fluoride) electrospun nanofibers for superhydrophilic and antibacterial properties. *Scientific Reports* **2019**, *9*, 383.

(52) Harkes, G.; Feijen, J.; Dankert, J. Adhesion of *Escherichia coli* on to a series of poly(methacrylates) differing in charge and hydrophobicity. *Biomaterials* **1991**, *12*, 853–860.

(53) Hogt, A. H.; Dankert, J.; Feijen, J. Adhesion of coagulase-negative staphylococci to methacrylate polymers and copolymers. *J. Biomed. Mater. Res.* **1986**, *20*, 533–545.

(54) Tang, Y. W.; Sussman, M.; Liu, D.; Poxton, Ia.; Schwartzman, J.; Merritt, A. Molecular Medical Microbiology, 2nd edition, 2014, Publisher: Academic Press, Tang, Yi-Wei, ISBN 9780123971692.

(55) Nguyen, T.; Roddick, F.A.; Fan, L. Biofouling of water treatment membranes: A review of the underlying causes, monitoring techniques and control measures. *Membranes* **2012**, *2*, 804–840.

(56) Al-Amshawee, S.; Yunusa, M. Y. B. M.; Lynam, J. G.; Lee, W. H.; Dai, F.; Dakhil, I. H. Roughness and wettability of biofilm carriers: A systematic review. *Environ. Technol. Innov*. **2021**, *21*, 101233.

(57) Zhang, Y. P.; Deng, L. L.; Zhong, H.; Pan, J. J.; Li, Y.; Zhang, H. Superior water stability and antimicrobial activity of electrospun gluten nanofibrous films incorporated with glycerol monolaurate. *Food Hydrocoll.* **2020**, *109*, 106116.

(58) De Cesare, F.; Di Mattia, E.; Zussman, E.; Macagnano, A. A 3D soil-like nanostructured fabric for the development of bacterial biofilms for agricultural and environmental uses. *Environ. Sci. Nano* **2020**, *7*, 2546–2572.

(59) Gupta, P.; Elkins, C.; Long, T. E.; Wilkes, G. L. Electrospinning of linear homopolymers of poly(methyl methacrylate): Exploring relationships between fiber formation, viscosity, molecular weight and concentration in a good solvent. *Polymer* **2005**, *46*, 4799–4810.

(60) Abdalla, S.; Obaid, A.; Al-Marzouki, F. M. Preparation and characterization of poly(vinylidene fluoride): A high dielectric performance nano-composite for electrical storage. *Results Phys.* **2016**, *6*, 617–626.

(61) Fischer, C. L. Antimicrobial activity of host-derived lipids. *Antibiotics* **2020**, *9*, 75.

(62) Kristmundsdottir, T.; Arnadottir, S. G.; Bergsson, G.; Thormar, H. Development and evaluation of microbicidal hydrogels containing monoglyceride as the active ingredient. *J. Pharm. Sci*. **1999**, *88*, 1011–1015.

(63) Shen, X.; Xie, T.; Wang, J.; Wang, F. Improved fouling resistance of poly(vinylidene fluoride) membrane modified with poly(acryloyl morpholine)-based amphiphilic copolymer. *Colloid Polym. Sci.* **2017**, *295*, 1211–1221.

Table Of Contents (TOC)